

Fırat Üniversitesi Deneysel ve Hesaplamalı Mühendislik Dergisi



Esnek Derz Bağlantı Detaylarının Betonarme Çerçevelerin Düzlem İçi Davranışına Etkisinin Nümerik Olarak İncelenmesi



¹İnşaat Mühendisliği Bölümü, Mühendislik Fakültesi, Manisa Celal Bayar Üniversitesi, Manisa, Türkiye.

¹taha.altiok@cbu.edu.tr

Geliş Tarihi: 26.07.2025

Walter Tarihi: 16.00.2025

Düzeltme Tarihi: 06.09.2025

doi: https://doi.org/10.62520/fujece.1751726

Kabul Tarihi: 16.09.2025 Duzenine Tarihi:06.09.2023 Araştırma Makalesi

Alıntı: A. Y. Altıok, "Esnek derz bağlantı detaylarının betonarme çerçevelerin düzlem içi davranışına etkisinin nümerik olarak incelenmesi", Fırat Üni. Deny. ve Hes. Müh. Derg., vol. 4, no 3, pp. 637-656, Ekim 2025.

Öz

Dolgu duvarlar, düzlem içi ve düzlem dışı etkiler altında kısa sürede hasar alarak yapısal sistem içerisindeki etkinliklerini kaybetmektedir. Bu nedenle, son yıllarda araştırmacılar, dolgu duvarların yapısal sistem üzerindeki etkilerini daha iyi anlamak ve bu elemanların sebep olduğu olumsuzlukları minimize edebilmek amacıyla alternatif bağlantı detaylarına odaklanmıştır. Bu çalışma, Türkiye Bina Deprem Yönetmeliği-2018 (TBDY-2018)'de önerilen esnek derz bağlantı detayını, özellikle düzlem içi davranış açısından sayısal olarak incelemeyi amaçlamaktadır. Bu detayın, düşük göreli kat ötelemesi seviyelerinde dolgu duvarlarının hasar görmesini önlemesi ve yapısal sistem üzerindeki olumsuz etkilerini azaltması hedeflenmektedir. Bu kapsamda, biri duvarsız (BF), biri rijit bağlı (IF-R) ve ikisi farklı kalınlıkta esnek derz bağlantılı (IF-F30 ve IF-F60) olmak üzere toplam dört betonarme çerçeve modeli oluşturulmuş; doğrusal olmayan Dynamic/Implicit (Quasi-Static) analizlerle tekrarlı ve tersinir yatay yükler altında performansları değerlendirilmiştir. Elde edilen bulgular, esnek derz bağlantılarının gerilme ve hasar dağılımını daha yayılı hale getirerek plastik şekil değiştirmeyi geciktirdiğini ve büyük göreli kat ötelemelerinde dahi sistemin taşıma kapasitesini koruduğunu göstermektedir. Ayrıca, esnek derz kalınlığının artırılmasının sünekliği olumlu etkilediği ve rijit dolgu bağlantısına kıyasla daha kararlı ve dengeli bir davranış sağladığı görülmüştür. Bu sonuçlar, esnek derz detaylarının yapısal tasarım sürecinde dikkate alınmasının, performans açısından önemli katkılar sunabileceğini ortaya koymaktadır.

Anahtar kelimeler: Dolgu duvar, Esnek derz, TBDY-2018, Hasar dağılımı, Düzlem içi davranış

^{*}Yazışılan yazar



Firat University Journal of Experimental and Computational Engineering



Numerical Investigation of the Effects of Flexible Joint Connection Details on the In-Plane Behavior of Reinforced Concrete Frames



¹Department of Civil Engineering, Faculty of Engineering, Manisa Celal Bayar University, Manisa, Türkiye.

¹taha.altiok@cbu.edu.tr

Received: 26.07.2025 Accepted: 16.09.2025 Revision: 06.09.2025 doi: https://doi.org/10.62520/fujece.1751726

Research Article

Citation: A.Y. Altıok, "Numerical investigation of the effects of flexible joint connection details on the in-plane behavior of reinforced concrete frames", First Univ. Jour. of Exper. and Comp. Eng., vol. 4, no 3, pp. 637-656, October 2025.

Abstract

Infill walls quickly become damaged under in-plane and out-of-plane effects, losing their effectiveness within the structural system. Therefore, in recent years, researchers have focused on alternative connection details to better understand the effects of infill walls on the structural system and to minimize the negative effects caused by these elements. This study aimed to numerically investigate the flexible joint connection detail recommended in the Türkiye Building Earthquake Code-2018 (TBEC-2018), focusing on in-plane behavior. This detail was intended to prevent damage to infill walls at low interstory drift levels and to mitigate their negative effects on the structural system. In this context, a total of four reinforced concrete frame models were created: one without walls (BF), one with rigid connections (IF-R), and two with flexible joint connections of varying thicknesses (IF-F30 and IF-F60). Their performance was evaluated under repeated and reversible lateral loads using nonlinear Dynamic/Implicit (Quasi-Static) analyses. The findings indicate that flexible joint connections delay plastic deformation by more evenly distributing stress and damage, while maintaining the system's load-bearing capacity even with large interstory drifts. Furthermore, increasing the flexible joint thickness was found to positively impact ductility and provide more stable and balanced behavior compared to rigid infill connections. These results demonstrate that considering flexible joint details in the structural design process can significantly contribute to performance.

Keywords: Infill wall, Flexible joint, TBEC-2018, Damage distribution, In-plane behavior

^{*}Corresponging author

1. Introduction

Infill walls are generally not considered part of the structural system and are included only as additional loads on the structure [1]. This approach can lead to inaccurate estimation of structural periods and, consequently, to the design of structures under unrealistic seismic loads. However, when the interaction of infill walls with the structural system is considered, numerous studies demonstrate their positive contribution up to collapse [2]. Some studies have determined that infill walls reduce the displacement of the frame system and column shear forces, while increasing the structure's lateral load-bearing capacity, overall strength, and base shear force [2-3]. In this context, numerous experimental and numerical studies examining the effects of the presence and absence of infill walls on the structural system are available in the literature. Dolšek and Fajfar [4] as well as Sattar and Liel [5] revealed that infill walls significantly increase the structural stiffness. Baghi et al. [6] similarly experimentally confirmed this increase in stiffness. Nwofor and Chinwah [7] stated that the displacement rates decreased in frames with infill walls. Ning et al. [8] investigated the effect of infill walls on the shear forces and plastic hinge formation in columns. Baghi et al. [6] emphasized that infill walls increase the bearing capacity and overall structural strength, and stated that this contribution should be included in structural models. Cavdar et al. [9] stated that different infill densities directly affect the seismic response of the structure. Usta et al. [10] investigated a building that had been subjected to an earthquake and showed that infill walls positively affected parameters such as building period, ground-floor shear, column bearing capacity, and interstory drift ratio, while also increasing base shear. These studies reveal only a partial impact of infill walls on structural behavior. Infill walls can lose their function due to in-plane and out-ofplane damage during earthquakes. Furthermore, even in small-scale earthquakes, damage to these walls can cause not only financial losses but also psychological effects by damaging users' confidence in the building. Following the devastating earthquakes, most notably the one centered in Kahramanmaras on February 6, 2023, numerous studies have specifically focused on the damage observed in infill walls and masonry structures [11-18]. Tan et al. [19] noted that while infill walls increase structural rigidity, performance indicators such as inter-story drifts can be negatively affected depending on earthquake records. Binici et al. [11] found that infill walls constructed with different block materials similar damage and that these materials did not have a significant advantage in terms of seismic performance. İnce [20] determined that serious damage occurred, especially on floors with large inter-story drifts and in walls that were not adequately connected to the frame. Yön et al. [21] stated that the lack of infill walls can lead to the formation of soft stories or weak stories, and that the degradation and thinning of the wall material lead to in-plane cracks.

In order to reduce the vulnerability of infill walls and increase their contribution to the structure, different strengthening techniques have been proposed in the literature [22]. Applications for strengthening infill walls are generally based on two basic approaches. The first approach aims to increase the structural strength of the walls, while the second approach is based on limiting the interaction between the wall and the supporting frame. Applications aimed at increasing the strength consider walls as active structural elements and generally provide significant gains in stiffness and bearing capacity. However, these methods can complicate the behavior of the system by increasing the interaction between the wall and the frame. Cases where the wall-frame interaction is ignored can lead to unexpected damage mechanisms and performance losses [23]. Tan et al. [24] stated that before the Kahramanmaras earthquakes, a structure strengthened as a hybrid with Fiber Reinforced Polymer (FRP) fabric and shear wall elements survived the earthquake without collapsing. Zargaran et al. [25] showed that walls strengthened using textile-reinforced mortar increased in-plane capacity by 53%. Triller et al. [26] reported that reinforcement with glass fiber-reinforced polyurethane provided strength up to 3.6% drift ratio without serious damage. Karimi and Mirjalili [27] compared different systems to increase out-of-plane capacity and emphasized that Glass Fiber Reinforced Polymer (GFRP) mesh and welded wire mesh systems are effective in high seismic regions. Shen et al. [28] reported that strengthening mud-filled walls used in traditional Chinese village houses with polypropylene mesh resulted in up to a 162% increase in out-of-plane capacity and improved ductility properties. Asad et al. [29] showed that spider web-like reinforcement systems provided a 31% increase in out-of-plane capacity and a 2.7-fold improvement in displacement. The second method, reducing the interaction between the infill wall and the frame, was included in the Türkiye Building Earthquake Code-2018 (TBEC-2018) [30], which came into force in Türkiye in 2018, after being included in the New Zealand [31] and United States [32] codes. Zhou et al. [33] experimentally investigated the out-of-plane mechanical behavior of flexibly connected masonry infill walls and reported that the best performance was achieved in the grid-beam form with a column spacing

of 2.5–3.0 m. Zhang et al. [34] aimed to reduce the frame-wall interaction with a flexible connection system and showed that in-plane damage was reduced and out-of-plane strength increased by over 100%. Zhang [35] compiled studies in this field, identified the main technical problems, and offered guidance for future research. Bayrak et al. [36] developed a flexible joint system, designing and numerically analyzing a structure where infill walls are independent of the frame. Analyses showed that the walls are independent of the frame in-plane and subjected to stress out-of-plane.

A review of the existing literature reveals that studies comprehensively addressing the effects of flexible connection details on in- and out-of-plane behavior are limited. This study numerically investigates the effects of flexible joint connection details, as defined in TBEC-2018, on in-plane behavior. Four different models were created using the finite element-based ABAQUS/CAE program: an empty frame, a rigidly connected frame with infill walls, and a frame with infill walls having two different flexible joint thicknesses. The models consisted of single-span, single-story reinforced concrete (RC) frames. Nonlinear dynamic implicit (quasi-static) analyses were performed for all models, and the analysis results were comprehensively evaluated in terms of lateral load bearing capacity, damage distribution, and stress behavior.

2. Wall Damages

Field observations reveal that infill walls in RC buildings are frequently damaged by earthquakes. Figure 1 presents various types of wall damage observed following the February 6, 2023 Kahramanmaraş-centered earthquake. Figure 1c illustrates a typical short column failure caused by discontinuity between the wall and the column due to the ribbon window configuration. Additionally, one of the most frequently observed damage types, in-plane cracking, is shown in Figure 1b–f, while out-of-plane damages are exemplified in Figure 1a–d–e. Cracks form at the frame-wall interfaces, particularly at low ground accelerations (PGA < 0.1 g); oblique cracks between 0.5 and 2 mm are observed in moderate ground motions. Under high ground accelerations, the combined in-plane and out-of-plane demands have led to wall collapse [11].

Infill walls exhibit similar behavior to RC shear walls under shear. However, reducing wall thickness and using low-strength materials like gypsum plaster reduces the shear capacity of these elements, facilitating crack formation. Furthermore, connecting wide-span and thin-section walls to the frame solely with mortar increases the risk of out-of-plane collapse, especially in the absence of beam support.

Infill walls, typically constructed of non-ductile materials, are among the earliest structural components to suffer damage during an earthquake. However, walls constructed with quality materials and good workmanship can contribute to the initial rigidity of the structure and absorb seismic energy, albeit to a limited extent. Otherwise, these elements pose a weak link in the structural system, threatening its integrity.

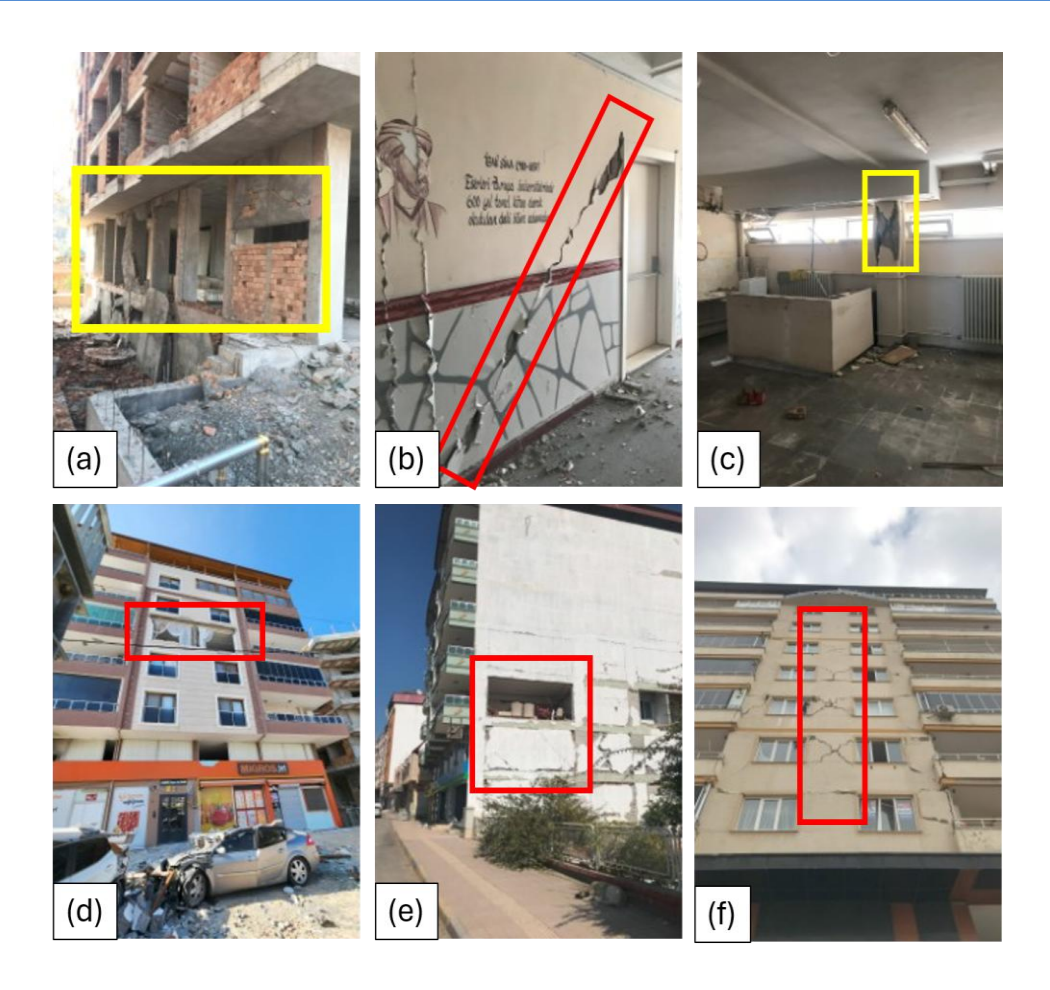


Figure 1. Wall damages

3. Flexible Joint Connection Detail Specified in TBEC-2018

Various structural separation strategies have been developed to simplify structural system behavior by reducing the interaction between the load-bearing system and infill walls and to prevent undesirable mechanisms such as soft stories, weak columns, and short columns. In this regard, the literature has suggested the separation of infill walls from the frame with horizontal or vertical sliding or deformable connections [37-39], the elimination of vertical connections [40], the use of plastic connectors in horizontal joints [41] and the use of polyurethane materials with high deformation capacity instead of mortar [42]. These approaches aim to limit the impact of infill walls on the structural system by reducing wall-frame interactions. However, if infill walls are completely separated from the structural system, there is a risk that these elements will separate from the frame and collapse during an earthquake. To prevent this risk and limit wall damage in small-scale earthquakes, TBEC-2018 [30], which entered into force in 2018, proposes a special solution that includes a flexible joint connection detail. In this detail, the first row of the wall is partially fixed to the frame with C-type profiles, providing out-of-plane stability and reducing wall-frame interaction. This prevents the wall from rigidly absorbing earthquake energy while also controlling the risk of collapse.

A schematic view of this connection detail proposed under TBEC-2018 [30] is presented in Figure 2. The regulation encourages the separation of infill walls from the structural system, provided their out-of-plane strength is maintained. If this connection type is used, the limit values specified by the regulation for relative story drifts can be relaxed by up to a factor of two.

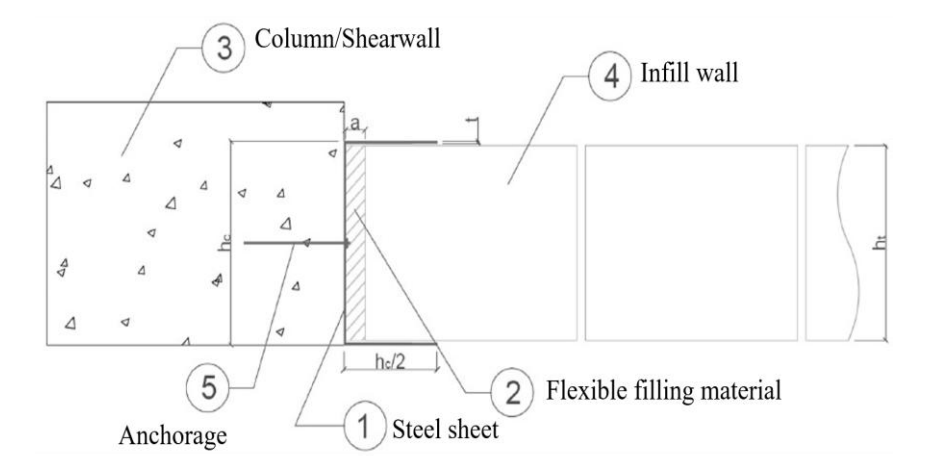


Figure 2. Illustration of the flexible joint connection detail as specified in TBEC-2018 [30]

4. Numerical Study

4.1. Finite element model

In this study, numerical analyses of RC frame systems were performed using ABAQUS/CAE [43] software. The models included a bare RC frame without an infill wall, a frame with a traditional infill wall, and flexible jointed walls of varying thicknesses. To ensure comparability, the same modeling approach and assumptions were applied in all cases.

RC elements, including their reinforcement, were modeled under full bond conditions. This bond definition was implemented with the "embedded region constraint" command. The infill walls, which were the focus of the study, were represented with a macro modeling technique. This approach enabled observation of overall system behavior rather than detailed local effects. The contact between the RC frame, the infill material, and the substrate (mineral wool-rock wool) was modeled using a surface-to-surface interaction definition. This allowed simulation of the compression behavior occurring within the flexible infill material. In the contact relationships, the RC frame and wall surfaces were defined as the master surface. The mineral wool interfaces were defined as the slave surface.

A nonlinear dynamic implicit (Quasi-Static) analysis method was applied in all analyses. The general geometric properties of the numerical models are presented in Figure 3. Each frame system was modeled as a single-story, single-span structure with dimensions of 3 m wide and 3 m high. Column and beam section dimensions were determined as 30 cm × 30 cm based on the TBEC-2018 regulation. The wall thickness, including plaster, was assumed to be 10 cm. The lower ends of the frame were defined as fixed supports; the foundation element was not included in the model to avoid increasing the mesh density. The thicknesses of the mineral wool layers placed between the infill wall and the frame were set to 30 mm and 60 mm. These corresponded to 1% and 2% of the story height, respectively. Thus, samples of the flexible joint system with different deformation capacities were evaluated together with their effects on the structural system response.

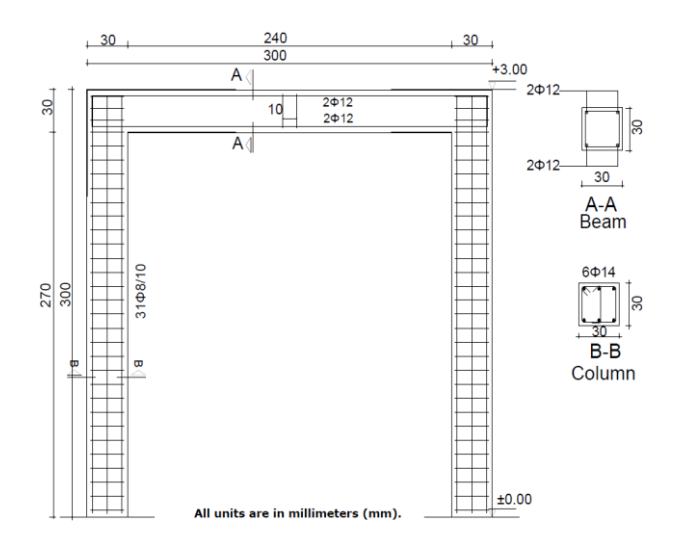


Figure 3. RC frame dimensions and reinforcement details

4.2. Finite element mesh

To improve model accuracy and maintain computational efficiency, a frequency-based convergence study was conducted on the RC frame system. In this context, the optimal element size was determined by comparing the natural frequencies corresponding to different mesh densities. To avoid unnecessary increases in computational time, mesh refinement was limited to levels that ensured adequate accuracy without excessively increasing the analysis duration. Figure 4 presents the graph of frequency values corresponding to the number of elements, while Figure 5 illustrates the meshed configuration of the model. As a result of the evaluations, C3D8R type eight-node reduced integration volume elements were preferred in the modeling. In the applied mesh layout, the RC frame has 5340 nodes and 3500 finite elements, with a selected mesh size of 60 mm.

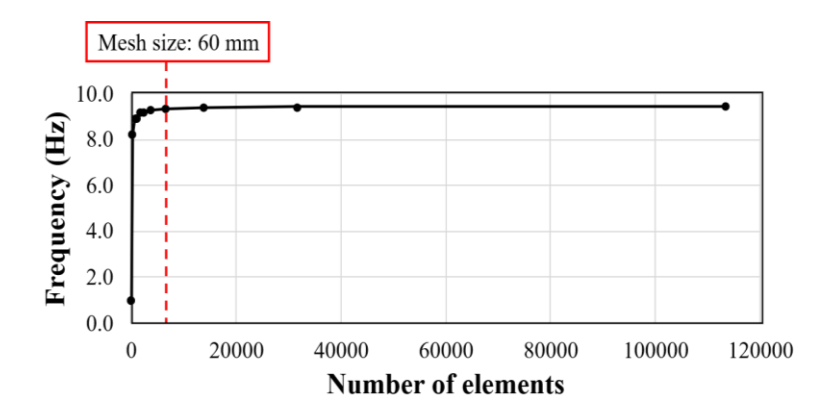


Figure 4. Convergence graph

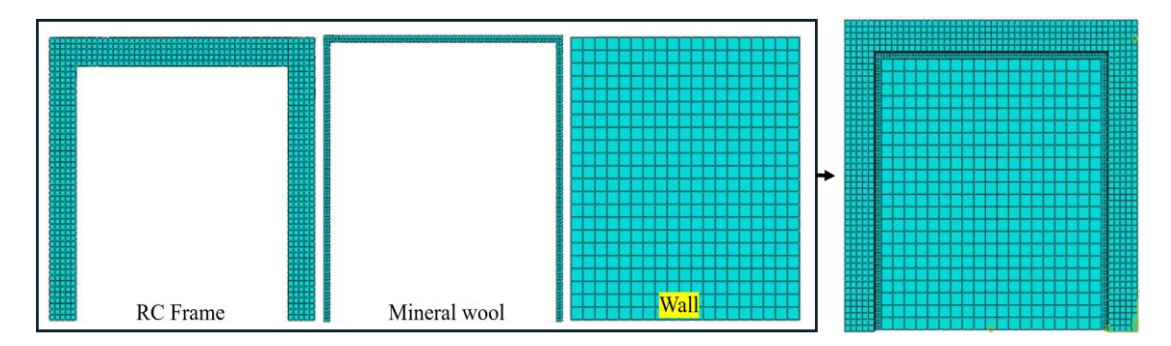


Figure 5. Mesh configurations

4.3. Boundary conditions and loading protocol

The foundation system was not included in the model to minimize analysis time and mesh density. Instead, the column bases were assumed to be fully fixed, and the support conditions were defined. Loading was applied horizontally at the midpoint of the beam and was repeated and reversible. To ensure consistency with the literature, the internationally widely used FEMA 461[44] standard was chosen as the loading protocol (Figure 6). Additionally, axial loads were applied to the tops of the columns, and these loads were determined to be approximately 15% of the load-bearing capacity of each column. This aimed to provide a realistic initial stress state for the frame.

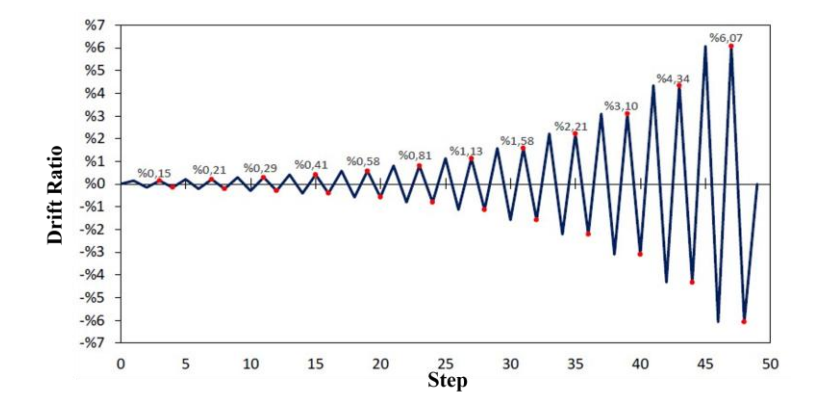


Figure 6. Loading protocol (FEMA 461 [44])

4.4. Material models and properties

In all models, the concrete strength of the RC system was assumed to be 30 MPa. The Concrete Damage Plasticity (CDP) material model was used to represent the nonlinear behavior of concrete and infill wall elements. The CDP model describes the plastic deformation, crushing under compression, and cracking under tension of concrete. Although initially developed to model the nonlinear mechanical response of concrete [45,46], it is reported in the literature that it can also be widely used in masonry wall elements with appropriate parameter adjustments [47]. The CDP model is based on two basic collapse mechanisms in concrete: cracking in tension and crushing under compression. Uniaxial tension and compression behavior are defined by two separate variables representing the damage that develops with plastic deformation: dt (tensile damage) and dc (compressive damage). These variables take values between 0 (undamaged state) and 1 (complete damage), depending on the equivalent plastic strain. The nonlinear behavior of the reinforcing steel was described with the Plasticity material model. This model is suitable for representing the nonlinear elastic behavior of ductile materials with high deformation capacity and was used to model the energy dissipation effect of the flexible joint system. The properties of the materials used in the structural models are presented in Tables 1-4.

Table 1. Elastic material properties

Material type	Young's modulus (MPa)	Poisson's ratio	Density (t/mm ³)
RC frame concrete	31800	0.2	2.4E-9
Wall	1612	0.2	2.2E-9
Reinforcement	210000	0.3	7.85E-9

Table 2. CDP material parameters [48]

Dilation	Eccentricity	f_{b0}/f_{c0}	K	Viscosity
Angle				Parameter
35	0.1	1.16	0.667	0.0058

Table 3. CDP material parameters of RC frame concrete

Compression behavior					Tension be	ehavior	
Yield stress	Inelastic	Damage	Inelastic	Yield stress	Cracking	Damage	Cracking
(MPa)	strain		strain	(MPa)	strain		strain
12	0.0	0.0	0.0	1.9200	0.0	0.0	0.0
24.3762	0.000123	0.5959	0.004067	0.4451	0.000523	0.7070	0.000365
30	0.000681	0.6635	0.004811	0.2906	0.000998	0.8530	0.001037
19.1250	0.002486	0.8508	0.009741	0.2201	0.001511	0.9290	0.003053
3.1717	0.013175	0.9381	0.021361	0.1937	0.001827	0.9500	0.005149

Table 4. CDP material parameters of infill wall

Compression behavior			Tension behavior				
Yield stress	Inelastic	Damage	Inelastic	Yield	Cracking	Damage	Cracking
(MPa)	strain		strain	stress	strain		strain
				(MPa)			
1.2	0.0	0.0	0.0	0.6797	0.0	0.0	0.0
2.4928	0.000174	0.5782	0.004791	0.7809	0.000046	0.6564	0.000959
3.0	0.001189	0.8085	0.010358	0.2785	0.001078	0.8168	0.003022
0.5745	0.010358	0.8715	0.015188	0.1162	0.005005	0.8649	0.005006
0.3004	0.019321	0.9098	0.021387	0.0875	0.007862	0.9000	0.007862

5. Results

In this study, four numerical models were developed to investigate the in-plane behavior of RC frames with and without infill walls and flexible joint details. The first model (BF) consists of a bare RC frame without any infill wall or joint detail. The second model (IF-R) represents a frame with a fully rigidly connected infill wall. The third (IF-F30) and fourth (IF-F60) models include infill walls with flexible joint thicknesses of 30 mm and 60 mm, respectively, as specified in TBEC-2018. These models were subjected to nonlinear analysis to evaluate their lateral load-carrying capacity, damage distribution, and stress behavior. The defined abbreviations will be used throughout the remainder of this section to distinguish between the models.

5.1. Lateral load-displacement behavior

The lateral load-displacement graphs of the models are shown in Figure 7, and the lateral load values and percentage changes obtained at 0.50% and 1% relative story drift ratios are given in Table 5. The reference model (BF) reached a lateral load bearing capacity of 4.92 kN at 0.50% drift and 6.65 kN at 1% drift. The IF-R model, in which the infill wall was incorporated into the frame with a rigid connection, reached the highest load bearing capacity of 45.92 kN at a 0.50% drift ratio, which was approximately 832.7% higher than the BF model. However, this value decreased to 39.58 kN at a 1% drift ratio, corresponding to an increase of 495.5% compared to BF. This shows that although the rigid infill connection is quite effective at low drifts, there is a relative decrease in bearing capacity as the deformation level increases.

When the models with flexible joints were investigated, the IF-F30 model with a 30 mm joint thickness showed increased by 583.8% in load capacity at 0.50% drift with 33.67 kN compared to the BF model, and increased by 503.4% in load capacity at 1% drift with 40.10 kN. These values demonstrate that the IF-F30 model can carry greater lateral loads than the rigid model at high drift ratios. On the other hand, the IF-F60 model with a 60 mm joint thickness showed increased by 399.6% in load capacity at 0.50% drift with 24.60 kN, and increased by 356.6% in load capacity at 1% drift with 30.34 kN. These results indicate that increasing

the flexible joint thickness significantly reduces the lateral load bearing capacity of the system. A thicker flexible joint limits the force transfer between the frame and the wall, reducing the contribution of the infill wall and therefore reducing the load bearing capacity of the structure.

Comparatively, the highest lateral load capacity was achieved in the IF-R model at a 0.50% drift ratio, while the highest capacity was observed in the IF-F30 model at a 1% drift ratio. This demonstrates that rigid connections are more advantageous for small deformations, but models with flexible connections can exhibit more stability as the drift increases. Furthermore, the load values closest to those in the BF model at both drift ratios were observed in the IF-F60 model, demonstrating that systems using thicker flexible joints behave almost like unfilled frames.

Since variations in lateral load capacity are directly linked to damage accumulation in the structural elements, the following section discusses the damage mechanisms of the frames under different infill configurations.

	Load v	Load values		ncrease rates
Model	Drift ratios		Drift ratios	
-	%0.5 (kN)	%1 (kN)	%0.5 (%)	%1 (%)
BF	4.92	6.65	0.0	0.0
IF-R	45.92	39.58	832.74	495.49
IF-F30	33.67	40.10	583.79	503.39
IE E60	24.60	30.34	300.63	356.56

Table 5. Lateral load values at different drift ratios and percentage changes

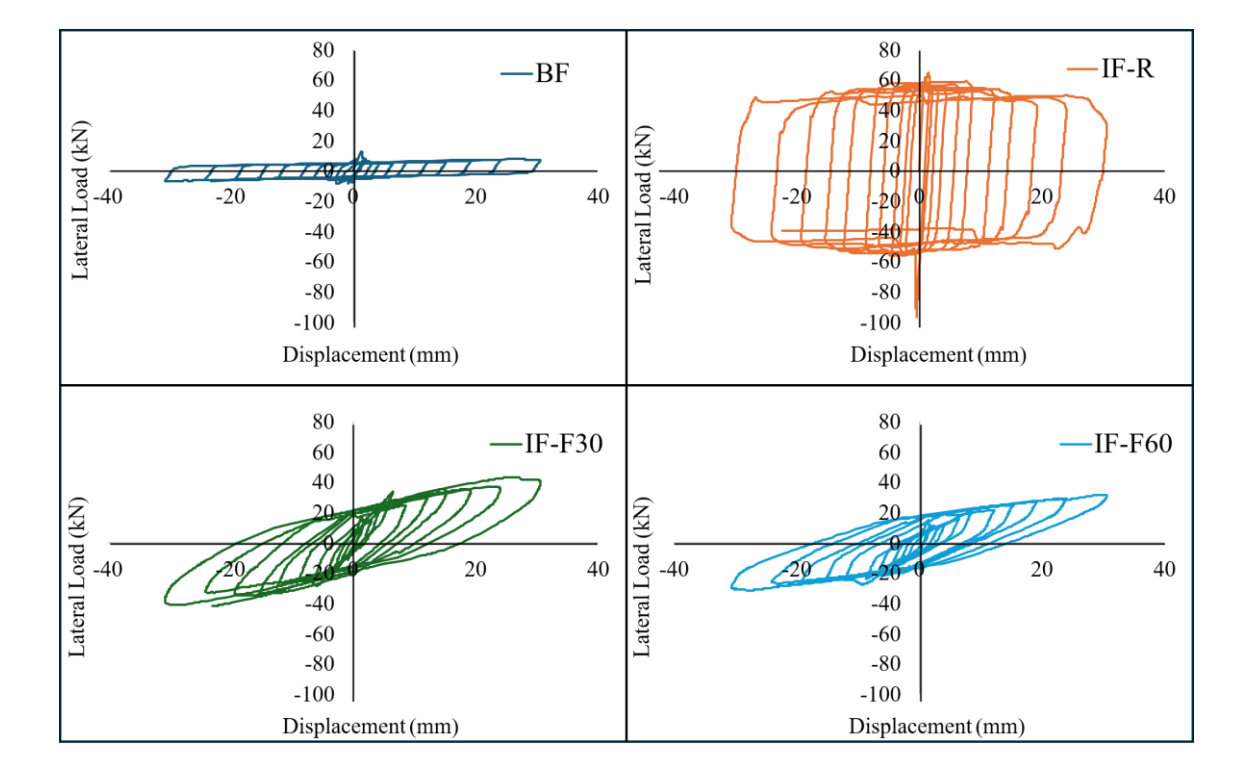


Figure 7. Load-displacement curves

5.2. Damage mechanism

This section only considers damage to RC frame elements; damage to infill wall materials is excluded. According to the findings presented in Table 6, 134 and 135 damaged elements were identified in the BF model, which consists of a plain frame. Comparisons made using this model as a reference revealed that the rigidly connected infill wall model (IF-R) exhibited damage increased by approximately 9.7% at 0.5% relative drift and increased by 56.3% at 1% drift. The 30 mm flexible joint model (IF-F30) exhibited damage

increased by 15.7% at 0.5% drift and increased by 40.7% at 1% drift. For the 60 mm flexible joint model (IF-F60), these increased by 11.2% and increased by 40.0%, respectively.

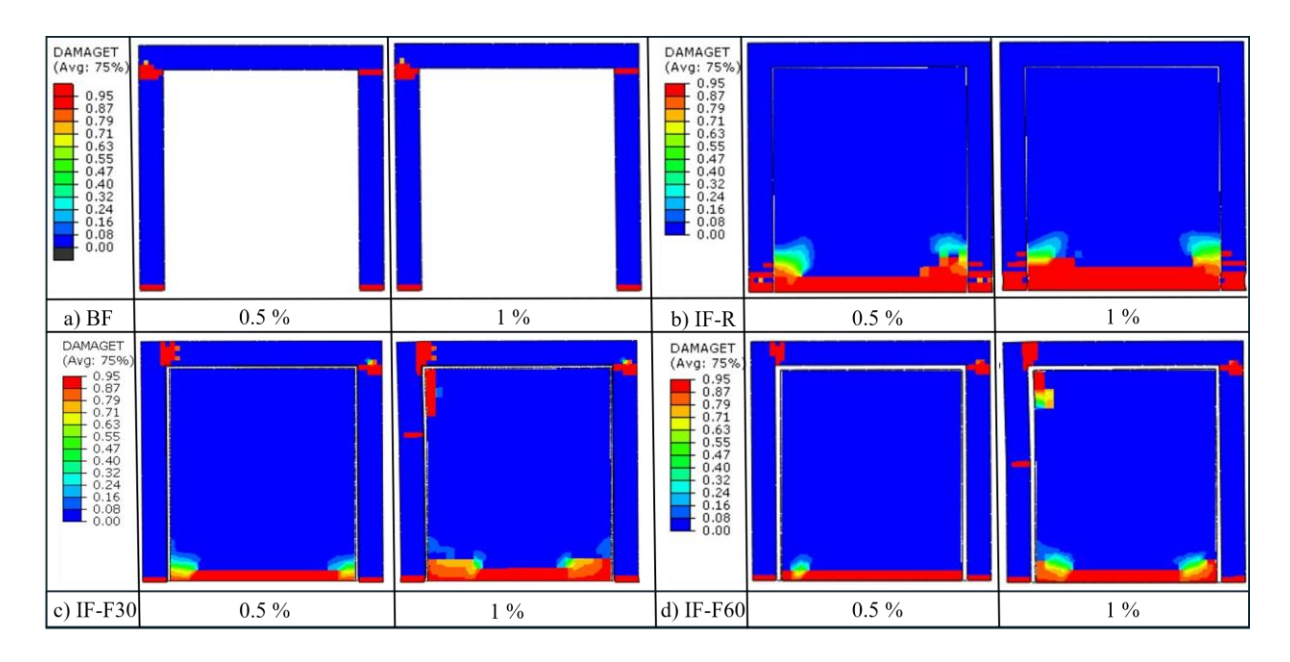
The results reveal that flexible joint details, compared to rigid connections, have a limiting effect on damage accumulation in frame elements, especially at the 1% drift ratio. Additionally, increasing the flexible joint thickness from 30 mm to 60 mm partially reduced the damage at the 1% drift ratio. This indicates that flexible joint thickness may be a determining parameter on structural behavior and damage formation at larger story drifts.

Table 6. Tensile damage in RC frame elements at different drift ratios and p	percentage changes

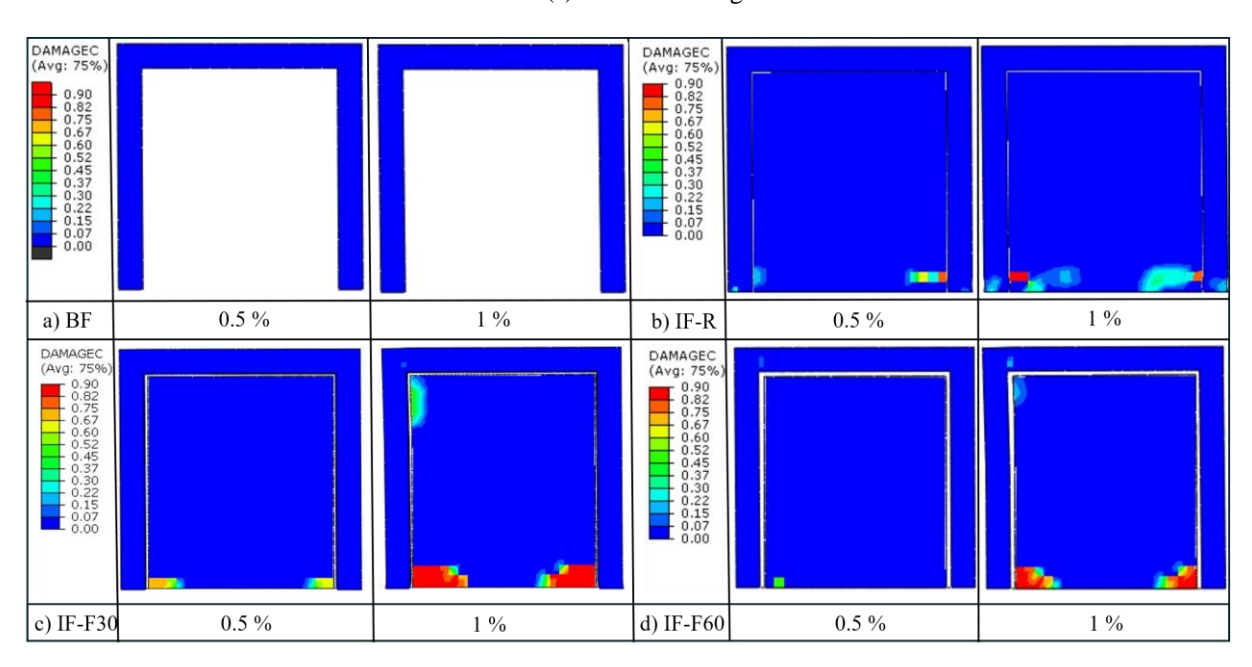
	Number of damaged elements Drift ratios		Damage increase rates		
Model			Drift ratios		
	%0.5	%1	%0.5 (%)	%1 (%)	
BF	134	135	0.0	0.0	
IF-R	147	211	9.7	56.3	
IF-F30	155	190	15.7	40.7	
IF-F60	149	189	11.2	40.0	

Figure 8a presents the tensile damage distributions obtained for four different models. The color scale indicates the severity of the tensile damage, with red tones indicating high damage regions. In the BF model, damage occurred in limited areas at 0.5% drift, with low-level damage observed particularly at the top connection and bottom ends of the column. At 1% drift, damage progressed to the bottom ends of both columns and the beam-column connection, concentrating on the plastic hinge regions of the system. In the IF-R model, at 0.5% drift, damage initiated at the wall-frame interaction zones, particularly at the bottom ends of the columns. At 1% drift, significant damage accumulation occurred at the bases of both columns, and mesh deterioration was observed in these areas. In the IF-F30 model, at 0.5% drift, damage initiated at the bottom ends of the columns and the bottom corner areas of the wall and spread to a limited extent. At 1% drift, the damage intensity in these regions increased. Damage was also observed at the wall corners and top joints. In the IF-F60 model, at the 0.5% drift ratio, damage was limited to the column base and the bottom corner of the adjacent wall. At the 1% drift ratio, increased damage was observed at the bottom ends of both columns and the bottom wall corners. Limited damage also occurred at the top wall joints. In the flexible joint models IF-F30 and IF-F60, a different damage distribution pattern was observed compared to the rigidly connected IF-R model. While the IF-R model exhibited concentrated damage initiating at the column base and rapidly propagating in that region, leading to severe localized failure, the flexible joint details allowed for a more uniform stress distribution. This prevented damage from accumulating at the column base and instead caused it to spread toward the beam ends, thereby reducing local damage intensity and enabling a more stable deformation behavior in the system.

Figure 8b presents the distribution of compressive damage in the RC members of the four models. In the BF model, no compressive damage occurred in the frame members at either drift ratio. In the IF-R model, limited compressive damage developed at the bottom ends of the columns at 1% drift. In the IF-F30 and IF-F60 models, no damage occurred at the column bases, while limited damage was observed at the beam ends.



(a) Tensile damage



(b) Compression damage

Figure 8. Damage developments

PEEQT (Tensile Equivalent Plastic Strain) represents plastic deformations occurring solely under tension. High PEEQT values reveal areas of the structure weakened by tension. Figure 9 shows the PEEQT distributions for four different models at 0.5% and 1% drift ratios. While no tensile plasticity occurred in the BF model at the 0.5% ratio, there were increases in plasticity at the 1% ratio, but these increases were limited. In the IF-R model, plasticity was observed at the frame-wall connections at both drift ratios. In the IF-F30 and IF-F60 models, the initial plasticity in the IF-R model was inhibited, and plasticity accumulation occurred at the 1% level, particularly at the column ends, but this did not reach significant levels.

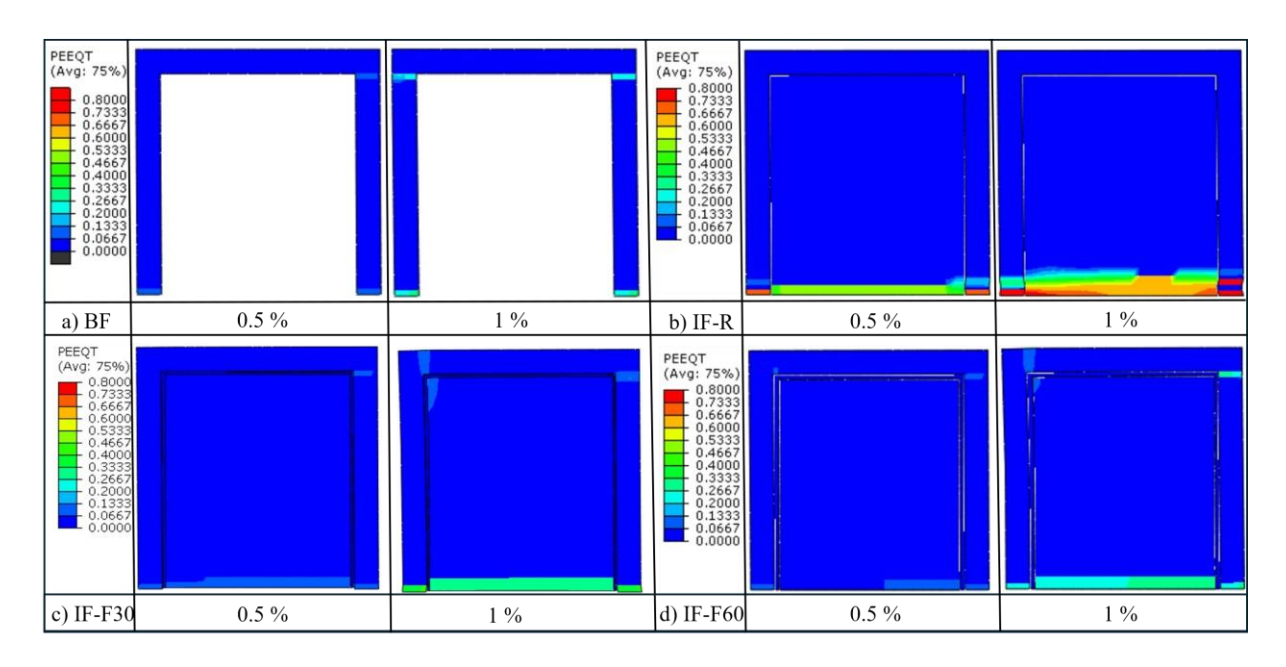


Figure 9. PEEQT distributions

PEEQ (Equivalent Plastic Strain) represents the equivalent plastic strain occurring at a material point. It indicates the amount of permanent deformation and is used to identify plastic hinge regions. High PEEQ values indicate regions where the structure begins to deform and dissipates energy through plastic deformation. Figure 10 shows the PEEQ distributions. In the BF model, plasticity is negligible at both drift ratios. In the IF-R model, local plastic strain occurred at the column bases and wall connections at a level of 1%. In the IF-F30 and IF-F60 models, plasticity was observed to be more limited and balanced, with local accumulation, particularly in frame elements, decreasing.

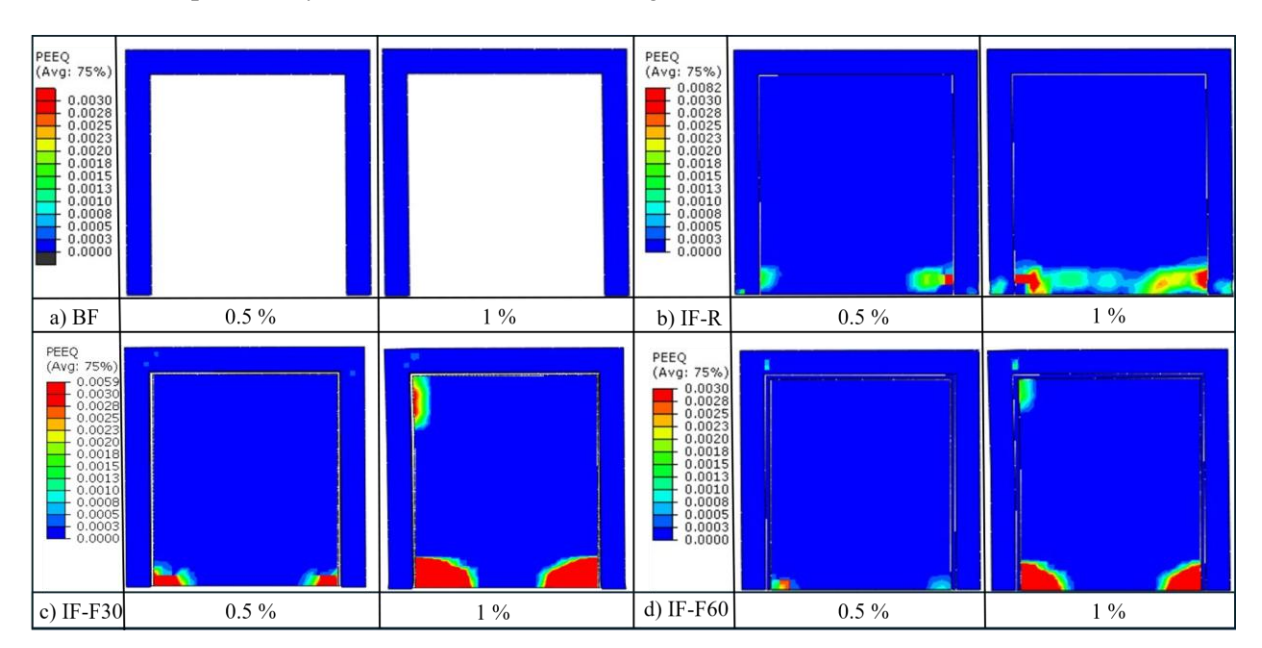


Figure 10. PEEQ distributions

5.3. Stress behaviors

This section discusses the instantaneous stress states and values of the models at 0.5% and 1% drift ratios under the loading effect. The values given in the tables represent the maximum stress in the local region at the moment of the relevant drift, not the entire system.

S, Mises, is the equivalent stress measure used to assess whether the material has reached its yield point under multiaxial stress conditions. It is an important indicator for identifying plasticization and structural strain zones. Table 7 and Figure 11 present the maximum S, Mises stress values for four different models at 0.5% and 1% drift ratios, along with their percentage increases compared to the BF model. In the BF model, stress values of 2.27 MPa and 1.85 MPa were obtained at 0.5% and 1% drift ratios, respectively. In the IF-R model, due to the effect of the rigid infill wall, S, Mises values increased by 127.3% at 0.5% drift and 174.6% at 1% drift. Significant stress accumulation was observed in the frame members in this model. In the IF-F30 model, stresses increased by 44.0% and 55.5% at 0.5% and 1% drift ratios, respectively. These increases were significantly lower than in the rigid model. In the IF-F60 model, the increased by were 42.3% (0.5%) and 57.8% (1%), which were similar to the IF-F30 model.

Stress increase rates Maximum stress value Model **Drift ratios Drift ratios** %0.5 (MPa) %1 (MPa) %0.5 (%) %1(%) BF 2.27 1.85 0.0 0.0 IF-R 5.16 5.08 127.3 174.6 44.1 IF-F30 3.27 2.88 55.5 IF-F60 3.23 2.92 42.3 57.8

Table 7. S, Mises stress values and percentage changes

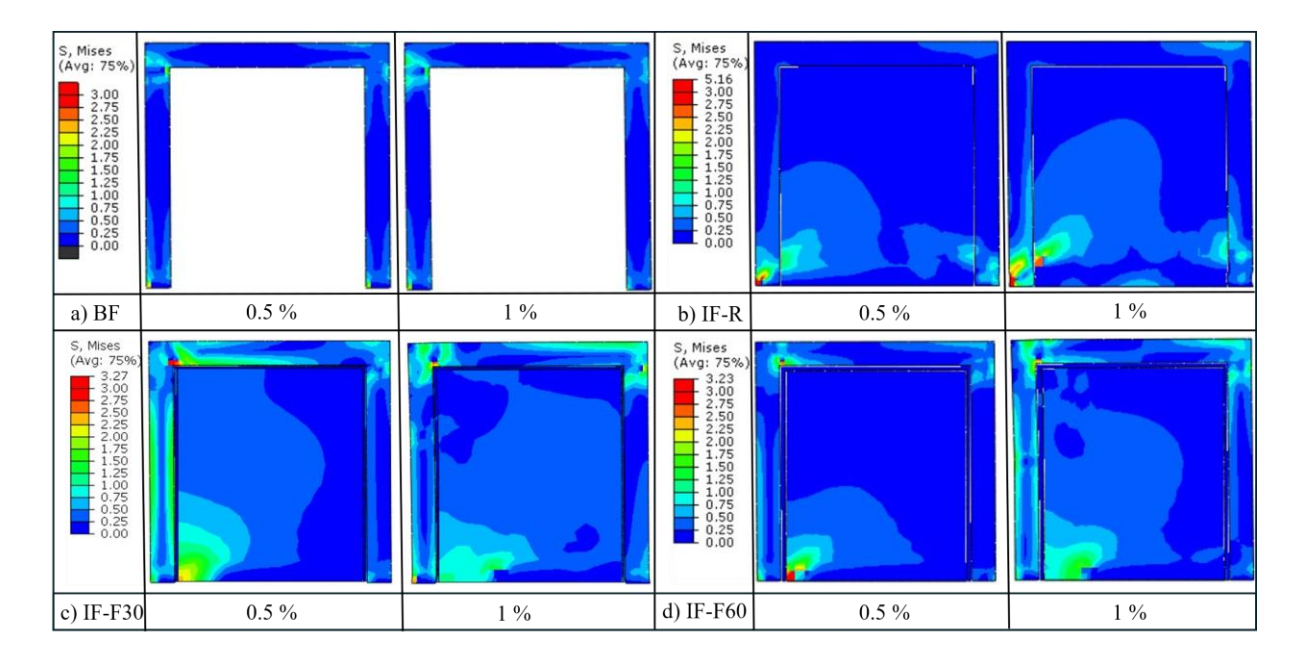


Figure 11. S, Mises stress distributions

S, Max Principal, indicates the stress accumulation in the regions of the structure subjected to tensile effect. It is particularly important for crack initiation and propagation. Table 8 and Figure 12 show the maximum principal stress (S, Max Principal) values at 0.5% and 1% drift ratios for four different models and their increased by percentages compared to the BF model. In the BF model, a stress of 1.32 MPa occurred at 0.5% drift, and 1.20 MPa occurred at 1% drift. In the IF-R model, these values increased by 5.3% (0.5%) and 22.5% (1%). In the IF-F30 model, the increased by 26.5% (0.5%) and 55.8% (1%), indicating a significant increase in tensile stress. In the IF-F60 model, similar increased by of 26.5% (0.5%) and 44.2% (1%) occurred. The instantaneous high tensile stresses observed in flexible joint models can be explained by the

delay in load transfer due to the absence of rigid connections and the increased relative movements in the frame elements.

Maximum stress value Stress increase rates Model Drift ratios **Drift ratios** %0.5 (MPa) %1 (MPa) %0.5 (%) %1(%) BF 1.32 1.20 0.0 0.0 22.5 IF-R 1.39 1.47 5.3 1.87 55.8 IF-F30 1.67 26.5 IF-F60 1.67 1.73 26.5 44.2

Table 8. S, Max Principal stress values and percentage changes

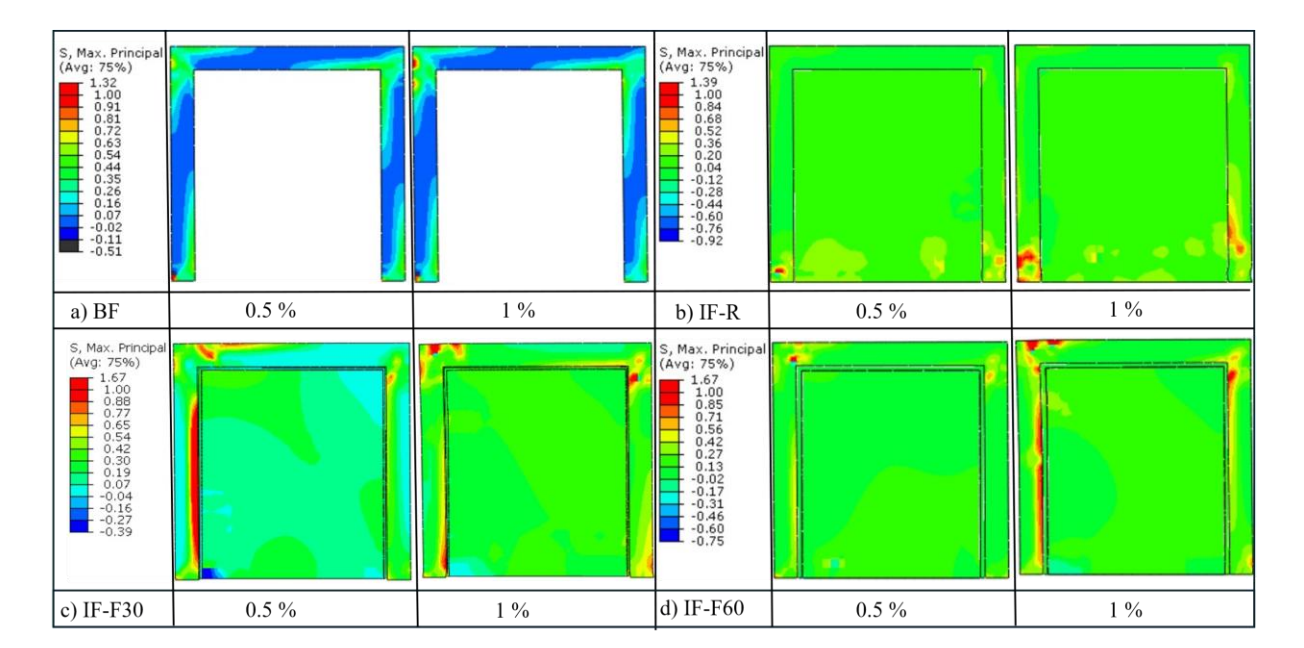


Figure 12. S, Max principal stress distributions

S, Min Principal, indicates the regions where the compressive effect is highest in the structure. The risk of crushing or local compressive damage is evaluated based on this component. Table 9 and Figure 13 show the minimum principal stress values at 0.5% and 1% drift ratios for four different models and their percentage increases compared to the BF model. In the BF model, values of -1.54 MPa were obtained at 0.5% drift, and -1.31 MPa at 1% drift. In the IF-R model, these values were -4.81 MPa and -4.82 MPa, respectively, increased by 212.3% and increased by 267.9% compared to the BF model. In the IF-F30 model, compressive stresses increased by 115.8% (0.5%) and 94.2% (1%). Similar increases were recorded in the IF-F60 model 117.5% (0.5%) and 126.7% (1%).

 Table 9. S, Min Principal stress values and percentage changes

	Minimum stress value		Stress increase rates		
Model	Drift 1	Drift ratios		ratios	
	%0.5 (MPa)	%1 (MPa)	%0.5 (%)	%1(%)	
BF	-1.54	-1.31	0.0	0.0	
IF-R	-4.81	-4.82	212.3	267.9	
IF-F30	-3.32	-2.54	115.8	94.2	
IF-F60	-3.35	-2.97	117.5	126.7	

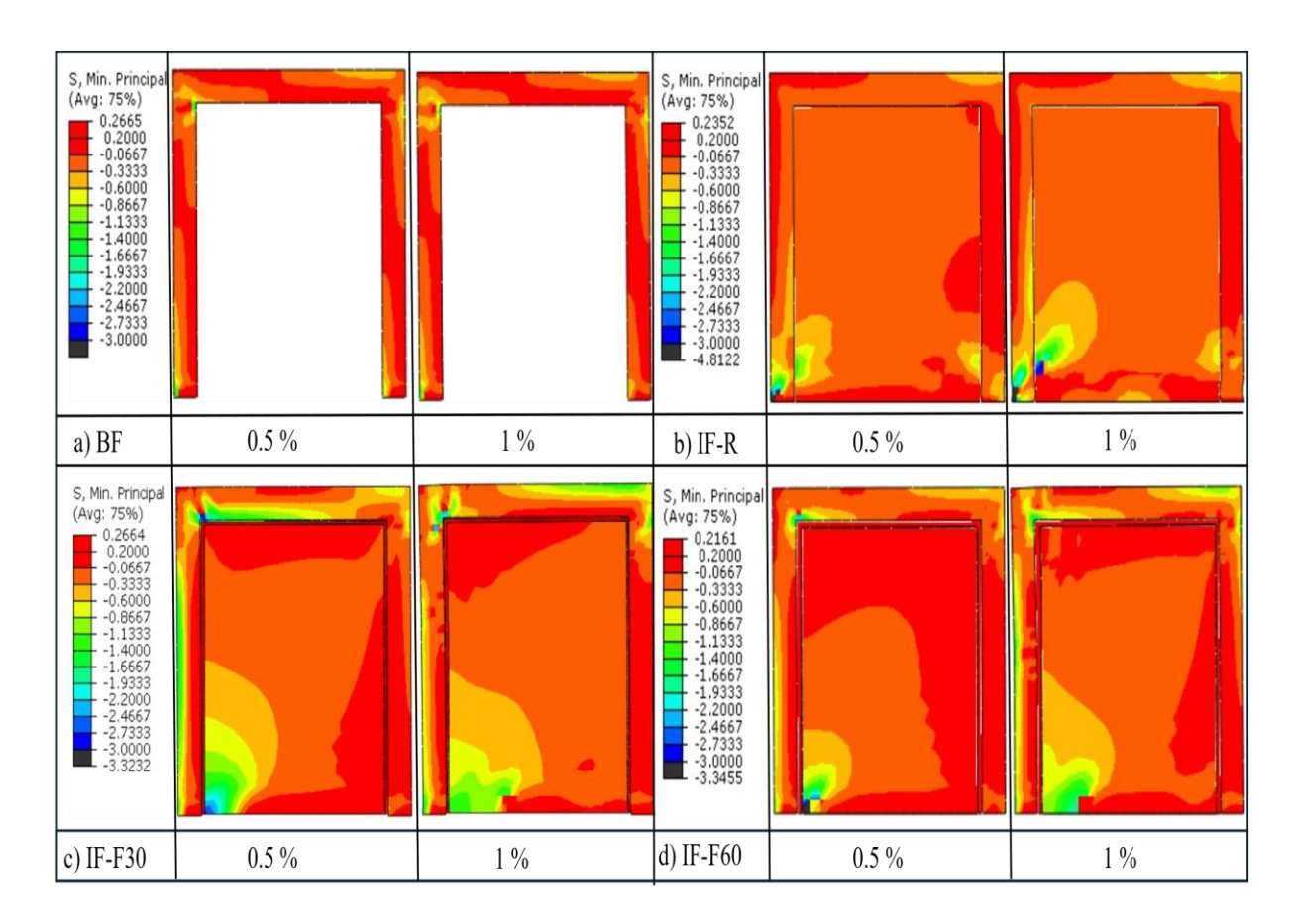


Figure 13. S, Min principal stress distributions

6. Conclusion

In this study, the effect of infill wall connection details on the in-plane behavior of RC frame systems was investigated using numerical methods. Four different structural systems were modeled and evaluated under nonlinear dynamic analyses: a bare RC frame (BF), a rigidly connected infill wall model (IF-R), and models with 30 mm and 60 mm flexible joint thicknesses (IF-F30 and IF-F60). The analyses were based on lateral load-carrying capacity, damage formation, and stress distribution at 0.5% and 1% drift ratios.

The findings indicate that rigidly connecting the infill wall to the frame provides a significant increase in lateral load capacity at low drifts, but this reduces the ductility of the system. In models with flexible joint connections, energy dissipation capacity was observed to develop in a more balanced and controlled manner. The IF-F30 model, in particular, performed better than the IF-R model at high drift ratios, demonstrating that flexible connections gain advantages as the deformation level increases. Additionally, it was understood that the increase in joint thickness reduces the bearing capacity of the system but positively affects the spread of damage and stress distribution.

The damage observed in models with flexible joints was more evenly distributed and controlled, with this effect becoming increasingly evident as joint thickness increased. In the rigid-connected model, the damage from compression was more localized and concentrated, while this effect was found to be more homogeneous throughout the frame in flexible details. In terms of plastic deformation behavior, it was determined that flexible joint models reduced local stress concentrations by dispersing plasticity due to tension, contributing to more stable system behavior.

Stress level assessments revealed that rigid infill connections caused significant stress concentrations in the frame elements, while flexible joint details distributed these stresses, contributing positively to the overall stability of the system. Mises stress levels were limitedly affected by changes in joint thickness, but flexible details made the stress distribution more homogeneous. No significant difference was observed in the

principal stress levels between the IF-F30 and IF-F60 models. In compressive stresses, the rigid model reached the highest values, while the flexible models limited these effects.

The results revealed that flexible joint connection details had a positive impact on in-plane structural behavior. These details were found to increase system safety and delay plastic deformation by more effectively dispersing stress and damage. Furthermore, it was observed that with the use of flexible joints, the structural behavior approached that of a bare frame, and even with larger inter-story drifts, the system maintained its load-bearing capacity, demonstrating stable performance. For future research, it is recommended to extend this investigation to multi-story buildings and to consider out-of-plane effects as well as long-term performance under repeated loading. Experimental validation of the proposed models would also strengthen the applicability of the findings.

7. Author Contribution Statement

Author 1 contributed to the conception of the idea, design of the study, literature review, evaluation of the results, supervision of the writing process, and critical revision of the manuscript for content.

8. Ethics Committee Approval and Conflict of Interest

- "There is no conflict of interest with any person/institution in the prepared article"
- "There is no need to obtain ethics committee permission for the prepared article"

9. Ethical Statement Regarding the Use of Artificial Intelligence

During the writing process of this study, the artificial intelligence tool "ChatGPT" developed by "OpenAI" was used only for limited purposes for linguistic editing. The scientific content, analysis and results belong entirely to the author.

10. References

- [1] M.M. Abdelaziz, M. S. Gomma, and H. El-Ghazaly, "Seismic evaluation of reinforced concrete structures infilled with masonry infill walls," Asian J. Civ. Eng., vol. 20, no. 7, pp. 961–981, Nov. 2019.
- [2] O. Akyürek, H. Tekeli, and F. Demir, "Plandaki Dolgu Duvar Yerleşiminin Bina Performansı Üzerindeki Etkisi," Int. J. Eng. Res. Dev., vol. 10, no. 1, Art. no. 1, Jan. 2017.
- [3] O. Oztürkoglu, U. Taner, and Y. Yesilce, "Investigation of infill wall-frame interaction in reinforced concrete structures," Dokuz Eylul Univ. Fac. Eng. J. Sci. Eng., vol. 17, no. 51, pp. 109–121, 2015.
- [4] M. Dolšek, and P. Fajfar, "The effect of masonry infills on the seismic response of a four-storey reinforced concrete frame a deterministic assessment," Eng. Struct., vol. 30, no. 7, pp. 1991–2001, Jul. 2008.
- [5] S. Sattar, and A. B. Liel, "Seismic performance of reinforced concrete frame structures with and without masonry infill walls," in Proc. 9th US Nat. 10th Can. Conf. Earthquake Eng., 2010, Accessed: Jul. 14, 2025.
- [6] H. Baghi, A. Oliveira, J. Valença, E. Cavaco, L. Neves, and E. Júlio, "Behavior of reinforced concrete frame with masonry infill wall subjected to vertical load," Eng. Struct., vol. 171, pp. 476–487, Sep. 2018.
- [7] T. Nwofor, and J. Chinwah, "Finite element modeling of shear strength of infilled frames with openings," Int. J. Eng. Technol., vol. 2, pp. 992–1001, Jun. 2012.
- [8] N. Ning, D. Yu, C. Zhang, and S. Jiang, "Pushover analysis on infill effects on the failure pattern of reinforced concrete frames," Appl. Sci., vol. 7, no. 4, Art. no. 4, Apr. 2017.
- [9] Ö. Çavdar, G. Köse, and F. Sunca, "Betonarme binaların deprem performanslarına dolgu duvarların etkisinin incelenmesi," Uludağ Univ. J. Fac. Eng., pp. 465–484, Apr. 2020.
- [10] P. Usta, Ö. Onat, and Ö. Bozdağ, "Effect of masonry infill walls on the nonlinear response of reinforced concrete structure: October 30, 2020 İzmir earthquake case," Eng. Fail. Anal., vol. 146, p. 107081, Apr. 2023.
- [11] B. Binici, A. Yakut, K. Kadas, O. Demirel, U. Akpinar, A. Canbolat, F. Yurtseven, O. Oztaskin, S. Aktas, and E. Canbay, "Performance of RC buildings after Kahramanmaraş Earthquakes: lessons toward performance based design," Earthq. Eng. Eng. Vib., vol. 22, no. 4, pp. 883–894, Oct. 2023.
- [12] B. Sevim, Y. Ayvaz, S. Akbulut, M. F. Aydıner, S. Uzun, and A. Ari, "Seismic performance and damage evaluation of reinforced concrete structures based on field investigation made after February 6, 2023, Kahramanmaraş Earthquakes," J. Earthq. Tsunami, vol. 18, no. 01, p. 2350032, Feb. 2024.
- [13] A. I. Turan, A. Celik, A. Kumbasaroglu, and H. Yalciner, "Assessment of reinforced concrete building damages following the Kahramanmaraş earthquakes in Malatya, Turkey (February 6, 2023)," Eng. Sci. Technol. Int. J., vol. 54, p. 101718, Jun. 2024.
- [14] M. Yetkin, İ. Ö. Dedeoğlu, and G. Tunç, "February 6, 2023, Kahramanmaraş twin earthquakes: Evaluation of ground motions and seismic performance of buildings for Elazığ, southeast of Türkiye," Soil Dyn. Earthq. Eng., vol. 181, p. 108678, Jun. 2024.
- [15] İ. Ö. Dedeoğlu, M. Yetkin, and Y. Calayir, "24 January 2020 Sivrice-Elazığ earthquake: Assessment of seismic characteristics of earthquake, earthquake territory and structural performance of reinforced concrete structures," Sak. Univ. J. Sci., vol. 26, no. 5, pp. 892–907, Oct. 2022.
- [16] İ. Ö. Dedeoğlu, M. Yetkin, Y. Calayır, and H. Erkek, "January 24, 2020 Sivrice-Elazığ (Türkiye) earthquake: The seismic assessment of the earthquake territory, geotechnical findings and performance of masonry buildings," Iran. J. Sci. Technol. Trans. Civ. Eng., vol. 48, no. 4, pp. 2393–2412, Aug. 2024.
- [17] M. Yetkin, İ. Ö. Dedeoğlu, and Y. Calayir, "24 Ocak 2020 Sivrice depremi sonrasında Elazığ ilinde bulunan minarelerde meydana gelen hasarların araştırılması ve değerlendirilmesi," Fırat Univ. J. Eng. Sci., vol. 33, no. 2, pp. 379–389, Sep. 2021.

- [18] I. O. Dedeoglu, M. Yetkin, G. Tunc, and O. E. Ozbulut, "Evaluating earthquake-induced damage in Dogansehir, Malatya after 2023 Kahramanmaras earthquake sequence: Geotechnical and structural perspectives," J. Build. Eng., vol. 104, p. 112266, Jun. 2025.
- [19] M. Tan, Ö. Avşar, F. Yıldızhan, and N. Atmaca, "Effect of infill walls on the seismic performance of a severely damaged substandard RC building during the February 6, 2023, Kahramanmaras earthquake sequence," Eng. Fail. Anal., vol. 169, p. 109117, Mar. 2025.
- [20] O. İnce, "Structural damage assessment of reinforced concrete buildings in Adıyaman after Kahramanmaraş (Türkiye) earthquakes on 6 February 2023," Eng. Fail. Anal., vol. 156, p. 107799, Feb. 2024.
- [21] B. Yön, İ. Ö. Dedeoğlu, M. Yetkin, H. Erkek, and Y. Calayır, "Evaluation of the seismic response of reinforced concrete buildings in the light of lessons learned from the February 6, 2023, Kahramanmaraş, Türkiye earthquake sequences," Nat. Hazards, vol. 121, no. 1, pp. 873–909, Jan. 2025
- [22] A. Furtado, H. Rodrigues, A. Arêde, and H. Varum, "Experimental tests on strengthening strategies for masonry infill walls: A literature review," Constr. Build. Mater., vol. 263, p. 120520, 2020.
- [23] M. H. Zhang, L. Pang, J. N. Ding, and D. Wang, "A review of the methods of strengthening RC frames with masonry infilled wall structures," Earthq. Eng. Eng. Vib., vol. 41, no. 1, pp. 53–62, 2021.
- [24] M. T. Tan, B. Binici, O. Kale, and G. Ozcebe, "The successful performance of a reinforced concrete building with FRP strengthened infill walls and externally installed shear walls subjected to Kahramanmaras and Hatay 2023 earthquakes," Bull. Earthq. Eng., Nov. 2024.
- [25] M. Zargaran, N. K. A. Attari, and N. Azadvar, "Seismic behavior of infill and nonstructural masonry walls strengthened with textile reinforced mortar," Constr. Build. Mater., vol. 458, p. 139691, Jan. 2025.
- [26] P. Triller, K. Kwiecień, A. Kwiecień, U. M. Tekieli, M. Szumera, T. Rousakis, V. Vanian, A.T. Akyildiz, and A. Viskovic, "Efficiency of FRPU strengthening of a damaged masonry infill wall under in-plane cyclic shear loading and elevated temperatures," Eng. Struct., vol. 317, p. 118652, Oct. 2024.
- [27] S. Karimi and M. R. Mirjalili, "Strengthened decoupled masonry infill walls: An experimental study on out-of-plane performance under cyclic loads," Constr. Build. Mater., vol. 475, p. 141159, May 2025.
- [28] Y. Shen, X. Yan, H. Jia, H. Liu, G. Wu, and W. He, "Experimental evaluation of the out-of-plane behavior of a traditional timber frame with mud and rubble infill wall strengthened by a polypropylene band mesh on one side," Structures, vol. 58, p. 105392, Dec. 2023.
- [29] M. Asad, J. Thamboo, T. Zahra, and D. P. Thambiratnam, "Mitigating damages to infill walls under combined in-plane and out-of-plane loadings using a spider web-inspired strengthening strategy: Numerical analyses," Eng. Struct., vol. 323, p. 119297, Jan. 2025.
- [30] TBEC-2018 Disaster and Emergency Management Agency (AFAD), Türkiye Building Earthquake Code, 2018.
- [31] NZS-4230, Design of Reinforced Concrete Masonry Structures. Standards New Zealand, 2004.
- [32] ACI 530.1-11, Building Code Requirements and Specification for Masonry Structures and Related Commentaries. American Concrete Institute, Farmington Hills, 2011.
- [33] X. Zhou, W. Zhao, P. Chen, D. Jin-peng, C. Chang-yun, and C. Kang, "Experimental and finite element analysis: Out-of-plane mechanical performance of infill walls with flexible connection," Adv. Struct. Eng., vol. 26, no. 8, pp. 1377–1394, Jun. 2023.
- [34] M. Zhang, J. Ding, W. Jin, K. Ding, and M. Ren, "Study on in-plane/out-of-plane seismic performance of masonry-infilled RC frame with openings and a new type of flexible connection," Bull. Earthq. Eng., vol. 22, no. 4, pp. 2201–2233, Mar. 2024.
- [35] H. Zhang, "A review of seismic performance of infill wall frame structures under flexible connections," Adv. Res. Teach., vol. 25, no. 1, pp. 13–20, 2024.
- [36] O. F. Bayrak, M. Bikçe, M. Erdem, and E. Emsen, "Dolgu duvarların düzlem içi ve düzlem dışı davranışına esnek derzli bağlantı elemanının etkisi," Osmaniye Korkut Ata Univ. J. Inst. Sci. Tech., vol. 3, no. 1, pp. 24–28, 2020.

- [37] X. Palios, M. N. Fardis, E. Strepelias, and S. N. Bousias, "Unbonded brickwork for the protection of infills from seismic damage," Eng. Struct., vol. 131, pp. 614–624, Jan. 2017.
- [38] M. Preti, and V. Bolis, "Masonry infill construction and retrofit technique for the infill-frame interaction mitigation: Test results," Eng. Struct., vol. 132, pp. 597–608, Feb. 2017.
- [39] P. Morandi, R. R. Milanesi, and G. Magenes, "Innovative solution for seismic-resistant masonry infills with sliding joints: In-plane experimental performance," Eng. Struct., vol. 176, pp. 719–733, Dec. 2018.
- [40] A. De Angelis, and M. R. Pecce, "The role of infill walls in the dynamic behavior and seismic upgrade of a reinforced concrete framed building," Front. Built Environ., vol. 6, Dec. 2020.
- [41]M. Vailati, and G. Monti, "Recycled-plastic joints for earthquake resistant infill panels," in Proc. 2nd Eur. Conf. Earthq. Eng. Seismol., Istanbul, 2014.
- [42] M. Gams, A. Kwiecien, J. Korelc, T. Rousakis, and A. Viskovic, "Modelling of deformable polymer to be used for joints between infill masonry walls and R.C. frames," Procedia Eng., vol. 193, pp. 455–461, 2017.
- [43] ABAQUS, User Assistance. Dassault Systèmes Simulia Corporation, Providence, Rhode Island, USA.
- [44]FEMA 461, Interim Testing Protocols for Determining the Seismic Performance Characteristics of Structural and Nonstructural Components. Federal Emergency Management Agency (FEMA), 2007.
- [45] J. Lubliner, J. Oliver, S. Oller, and E. Onate, "A plastic-damage model for concrete," Int. J. Solids Struct., vol. 25, no. 3, pp. 299–326, 1989.
- [46] J. Lee, and G. L. Fenves, "Plastic-damage model for cyclic loading of concrete structures," J. Eng. Mech., vol. 124, no. 8, pp. 892–900, 1998.
- [47] M. Valente, and G. Milani, "Damage assessment and collapse investigation of three historical masonry palaces under seismic actions," Eng. Fail. Anal., vol. 98, pp. 10–37, 2019.
- [48] A. Raza, and A. Ahmad, "Numerical investigation of load-carrying capacity of GFRP-reinforced rectangular concrete members using CDP model in ABAQUS," Adv. Civ. Eng., vol. 2019, 2019.